Received: 4 May 2020 | Revised: 28 January 2021 | Accepted: 11 March 2021

DOI: 10.1111/jnc.15349

ORIGINAL ARTICLE

Journal of Neurochemistry JNC The Official Journal of the International Society for Neurochemistry WILEY

CD33M inhibits microglial phagocytosis, migration and proliferation, but the Alzheimer's disease-protective variant CD33m stimulates phagocytosis and proliferation, and inhibits adhesion

Claire Ann Butler[1,2] | Peter Thornton[2] | Guy Charles Brown[1]

[1]Department of Biochemistry, University of Cambridge, Cambridge, UK

[2]AstraZeneca, Cambridge, UK

Correspondence
Guy Charles Brown, Department of Biochemistry, University of Cambridge, Cambridge, CB2 1QJ, UK.
Email: gcb3@cam.ac.uk

Funding information
Biotechnology and Biological Sciences Research Council; Medical Research Council, Grant/Award Number: MR/L010593; Innovative Medicines Initiative 2 Undertaking, Grant/Award Number: 115976

Abstract

CD33 is a Siglec (sialic acid-binding immunoglobulin-type lectin) receptor on microglia. Human CD33 can be alternatively spliced into two isoforms: the long isoform (CD33M) and a shorter isoform (CD33m) that lacks the sialic acid-binding site. CD33m appears to protect against Alzheimer's disease; however, it remains unclear how. To investigate potential mechanisms by which CD33m may confer protection, we expressed the CD33m and CD33M isoforms of human CD33 in mouse BV-2 and human CHME3 microglial cells and assessed microglia functions. In the BV-2 cells, CD33M inhibited microglial phagocytosis of beads, synapses, debris and dead cells, while CD33m increased phagocytosis of beads, debris and cells. RNAi knockdown of the endogenous mouse CD33 increased phagocytosis and prevented CD33m's (but not CD33M's) effect on phagocytosis. CD33M increased cell attachment but inhibited cell proliferation, while CD33m did the opposite. We also found that CD33M inhibited cell migration. In human CHME3 cells, CD33M increased cell attachment, but inhibited phagocytosis, proliferation and migration, whereas CD33m did the opposite. We conclude that CD33M inhibits microglial phagocytosis, inhibits migration and increases adhesion, while CD33m increases phagocytosis, proliferation and inhibits adhesion. Thus, CD33m might protect against Alzheimer's disease by increasing microglial proliferation, movement and phagocytosis of debris and dead cells.

KEYWORDS

Alzheimer's disease, CD33, Microglia, Neuroinflammation, Siglec-3

Abbreviations: AD, Alzheimer's disease; Aβ, amyloid beta; BSA, bovine serum albumin; CD33, cluster of differentiation 33; CD33M, long form of CD33 including exon 2; CD33m, short form of CD33 excluding exon 2; DAPI, 4',6-diamidino-2-phenylindole; DMEM, Dulbecco's Modified Eagle's Medium; ECM, extracellular matrix; EGFP, enhanced green fluorescent protein; FACS, fluorescence-activated cell sorting; FBS, foetal bovine serum; GFP, green fluorescent protein; ITAM, immunoreceptor tyrosine-based activation motif; ITIM, immunoreceptor tyrosine-based inhibition motif; K7R-CD33, CD33M with a K7R mutation; PBS, phosphate-buffered saline; PFA, paraformaldehyde; PNA, peanut agglutinin; siglec, sialic acid-binding immunoglobulin-type lectins.

1 | INTRODUCTION

Microglia are brain-resident macrophages and can phagocytose pathogens, debris, protein aggregates, apoptotic cells, neurons and synapses (Galloway et al., 2019; Vilalta & Brown, 2018; Wolf et al., 2017). Microglial phagocytosis is mediated and regulated by several different receptors, including CD33. Human CD33 (also known as Siglec-3) is a transmembrane receptor with an extracellular domain that binds sialic acid residues of glycoproteins on the cell surface, and uses an intracellular ITIM (immunoreceptor tyrosine-based inhibition motif) domain and ITIM-like domain to inhibit immune/inflammatory functions of cells (Estus et al., 2019; Paul et al., 2000). CD33 is expressed on myeloid cells, including microglia, monocytes, dendritic cells and peripheral macrophages (Crocker & Varki, 2001). In such cells, extracellular cross-linking using antibodies induces tyrosine phosphorylation of the ITIM and ITIM-like domains of CD33, which in turn recruits and activates the tyrosine phosphatases SHP-1 and SHP-2, resulting in inhibition of tyrosine phosphorylation signalling in the cells (Paul et al., 2000; Taylor et al., 1999; Ulyanova et al., 1999).

Human CD33 and mouse CD33 are homologous in their extracellular domains, but have limited homology in their intracellular domains, such that mouse CD33 has an ITIM-like domain, but lacks the ITIM domain present on human CD33 (Brinkman-Van der Linden et al., 2003). Griciuc et al. (2013) reported that both human and mouse CD33 inhibited phagocytosis of amyloid beta (Aβ). Whereas Bhattacherjee et al. (2019) reported that expression of human CD33 inhibited monocyte and microglial phagocytosis (of beads, dextran, myelin and Aβ), but expression of mouse CD33 had no effect on phagocytosis. These results appear inconsistent, so it remains unclear whether mouse CD33 has a similar function to human CD33.

Human CD33 can be alternatively spliced into two major isoforms known as CD33M (also known as FL-CD33), which encodes the full-length protein (containing all seven exons), whereas CD33m (also known as D2-CD33 or CD33ΔV-Ig), the shorter form, lacks the sialic acid-binding domain coded by exon 2 (Hernández-Case Iles et al., 2006). Mouse CD33 can also be alternatively spliced into two isoforms but this occurs in the cytoplasmic region and therefore the isoforms are distinct from those in human CD33 (Tchilian et al., 1994). GWAS studies have identified a single-nucleotide polymorphism (SNP, rs3865444A) with decreased risk of Alzheimer's disease (AD) (Bradshaw et al., 2013; Hollingworth et al., 2011; Malik et al., 2013; Naj et al., 2011). Subsequently it was found that rs3865444 (in the promotor of CD33) is in linkage equilibrium with rs12459419 (which is located in the intron close to the start of exon 2 of CD33), and this may be the disease-modifying site by increasing the splicing out of exon 2, thus decreasing the ratio of CD33M to CD33m (Estus et al., 2019). However, the underlying biology of why CD33m and CD33M confer differing susceptibility to developing Alzheimer's disease remains unclear.

One hypothesis is that CD33M inhibits microglial uptake of Aβ, while CD33m is non-functional and therefore does not inhibit phagocytosis of Aβ, resulting in increased Aβ uptake, reduced amyloid plaque load and disease (Bradshaw et al., 2013; Griciuc et al., 2013). Griciuc et al. (2013) found increased microglial expression of CD33M in Alzheimer's brains, and a positive correlation between microglial expression of CD33M and plaque load, suggesting that CD33M inhibits microglial phagocytosis of plaques. Consistent with this, CD33 knockout mice crossed with an amyloid model (APP/PS1) had reduced plaque load. Furthermore, Griciuc et al. (2013) showed that microglia from CD33 knockout mice took up more Aβ, indicating that endogenous mouse CD33 inhibited microglial uptake of Aβ. They also reported that over-expression of human CD33M in BV-2 microglial decreased Aβ uptake, while expression of human CD33m had no effect on Aβ uptake (Griciuc et al., 2013).

Bradshaw et al., (2013) compared humans with the risk and protective alleles of CD33, and found that the risk allele for AD was associated with: increased surface expression of CD33M on monocytes, decreased Aβ uptake by monocytes and increased fibrillar Aβ in both live brain and post-mortem brains. The post-mortem brains had increased neuritic pathology and activated microglia (Bradshaw et al., 2013). Overall, these findings and those of Griciuc et al. (2013) are consistent with the hypothesis that the protective allele increases expression of CD33m relative to CD33M, and that CD33M inhibits microglial phagocytosis of Aβ, while CD33m is non-functional, potentially explaining why CD33M expression is detrimental in AD, whereas CD33m is protective.

The above model assumes that CD33m has lost function compared to CD33M. However, recently a variant of the CD33 gene was found resulting in no CD33 expression and no change in AD risk. This finding is not consistent with CD33m being protective simply by loss of CD33M function, and therefore suggests the possibility that CD33m might gain some unknown function relative to CD33M to protect against AD (Estus et al., 2019; Papageorgiou et al., 2019).

Here, we sought to elucidate the roles of CD33 in microglial function and AD by determining: (1) whether CD33M and CD33m have differential effects on microglial phagocytosis of a variety of different phagocytic targets, including different forms of Aβ, (2) whether CD33 variants affect microglial migration, attachment and proliferation, (3) whether CD33m has a loss-of-function or gain-of-function effect on microglia, (4) whether mouse and human CD33 have different effects on microglia functions, and finally (5) whether human CD33 has different effects on mouse and human cells. To address these aims, we expressed human CD33M and CD33m in mouse and human microglial cell lines (BV-2 and CHME3 respectively) and measured microglial functions, such as phagocytosis, migration, attachment and proliferation.

2 | MATERIALS AND METHODS

2.1 | Ethical statement

Explicit institutional ethical approval was not required for this study. The ARRIVE guidelines were not applied since no animals are involved.

2.2 | Study design

This study was not pre-registered and no randomisation, blinding or sample calculation was performed. The study was exploratory and no exclusion criteria were pre-determined. For all experiments, unless stated otherwise, at least $n = 3$ independent cell culture preparations were used.

2.3 | Cell culture and lentiviral transfection for stable cell line generation

BV-2 cells (RRID:CVCL_0182, ECACC) and CHME3 cells (RRID:CVCL_II76, a gift from Dr Svetlana Khoronenkova, who got them from Dr Brian Bigger, who got them from the originator Prof Marc Tardieu) were cultured in DMEM (Life Technologies, 41965039), supplemented with 10% heat-inactivated foetal bovine serum (FBS, Life Technologies, 10500064) and 1% penicillin/streptomycin (Sigma, P4333). Cells were cultured in pre-coated, cell culture treated 75 cm^2 (T75) flasks and the attaching population of the cells were used for all experiments. Maximum passage used for BV-2 and CHME3 lines was 25.

For lentivirus generation packaging, psPAX2, and envelope, psMD2.G, plasmids were a gift from David Allendorf, University of Cambridge. The CD33m, CD33M and CD33-K7R transfer plasmids were a gift from Dr Roland Walter of Fred Hutchinson laboratory, Seattle. EGFP only (control) transfer plasmid was sourced from Addgene (RRID:Addgene_12254). All three plasmids were combined according to Addgene lentiviral production protocol and transfected into HEK 293 (RRID:CVCL_0045, ECACC) cells using polyethylenimine (PEI, Sigma, 408727) transfection reagent. HEK 293 cells were cultured in DMEM/F12 with GlutaMAX media (Life Technologies, 31331093), supplemented with 10% heat-inactivated FBS and 1% penicillin/streptomycin. Maximum passage for HEK 293 used was 25. After 24 hr, media were exchanged. After a further 24 hr, media were harvested, centrifuged and filtered through a 0.45-micron filter. These media (containing lentiviral particles) were then added to BV-2 cells at 50%–60% confluency with the addition of 8 μg/mL polybrene (Merck, TR-1003-G). After 18 hr, cells were harvested and EGFP expression was assessed using flow cytometry (Accuri C6, BD systems). Cells that were positive for EGFP were FACS (Aria III) sorted collecting only the highest 25% of EGFP-expressing cells, and therefore the highest CD33M, CD33m or K7R-CD33 M expressing cells, for future experiments.

For generation of human neuronal debris for CHME3 phagocytosis experiments, human SH-SY5Y (RRID:CVCL_0019) cells were cultured in T75 flasks in DMEM/F12 with GlutaMAX media supplemented with 10% heat-inactivated FBS and 1% penicillin/streptomycin. Maximum passage for SH-SY5Y cells was 25. None of the cell lines used are a commonly misidentified cell line; however, they have not been authenticated.

2.4 | RNAi knockdown of mouse CD33 M

Cells were seeded at 300,000 per well in six-well plate in DMEM supplemented with 10% heat-inactivated FBS and 1% penicillin/streptomycin. After 24 hr, cells were subjected to RNAi:lipid mix containing 60 pmol CD33 targeting (Thermofisher, 4390771) or non-target (scrambled RNAi) (Thermofisher, 4390843) and 3% (v/v) lipofectamine 3000 (Thermofisher, L3000008) in serum-free opti-MEM media (Invitrogen, 51985). After 3-hr incubation at 37°C, transfection media were removed and replaced with DMEM supplemented with 10% heat-inactivated FBS and 1% penicillin/streptomycin. After a further 24 hr, cells were harvested using trypsin (Life Technologies, 15400054) and seeded into phagocytosis plates either 96-well or 24-well plates, assay depending, in DMEM supplemented with 0.5% heat-inactivated FBS and 1% penicillin/streptomycin. Phagocytosis assays were typically performed 24 hr later.

2.5 | RNA extraction and qPCR

Whole RNA was extracted using Monarch total RNA Miniprep kit (NEB, T2010). cDNA was synthesised using 1 μg of whole RNA, Superscript II Transcriptase kit (Invitrogen, 18064022) and random hexamer primers (ThermoFisher, SO142). qPCR was performed using SYBR Green JumpStart Taq ReadyMix (Sigma, S4438). Amplification was performed using Rotor-gene Q cycler (Qiagen). Data were analysed using rotor-gene software and data expressed as comparative concentration which was normalised to GAPDH house-keeping gene for BV-2 cells or 18s rRNA for CHME3 cells. Primer sequences for human CD33 M (forward, TGGCTATGGATCCAAATTTCTGGCTG; reverse, AGCATAATGCAGCTCCTCATC) and human CD33m (forward, CCTGCTGTGGGCAGACTTGAC; reverse, AGCATAATGCAGCTCCTCATC), human 18s rRNA (forward, GGCCCTGTAATTGGAATGAGTC; reverse, CCAAGATCCAACTACGAGCTT), mouse GAPDH (forward, GTTGTCTCCTGCGACTTCA; reverse, GGTGGTCCAGGGTTTCTTA) and mouse CD33 M (forward, ATGAGAGAGCTGGTCCTGGT; reverse, CCCATGTGCACTGACAGCTT).

2.6 | Cell surface staining of mouse CD33 after RNAi knockdown

BV-2 cells were harvested using trypsin and pelleted. BV-2 cells were resuspended in flow cytometer staining solution (Invitrogen, 00-4222-57). BV-2 cells were then stained with either rat anti-IgG1 isotype control (RRID:AB_470047, ThermoFisher) or rat anti-mouse CD33 (RRID:AB_2637179, ThermoFisher) both directly conjugated to phycoerythrin (PE) and diluted 1:50 (working concentration of 4 μg/ml) in staining solution at 4°C for 30 min, to prevent receptor internalisation. All cells were washed with 1X PBS and phycoerythrin (PE) fluorescence quantified using flow cytometer (Accuri C6, BD systems).

2.7 | Cell surface staining of human CD33 variants

Cells were harvested using trypsin and pelleted. Cells were re-suspended in flow cytometer staining solution (Invitrogen, 00-4222-57). For both BV-2 and CHME-3 CD33 over-expressing cell lines mouse anti-IgG1 isotype control (BioLegend, 400114) was used. For detection of human CD33M and K7R-CD33M mutant in both BV-2 and CHME3s, mouse anti-human CD33 (clone h67.6) (RRID:AB_2566107, BioLegend) was used. Both the isotype control and anti-human CD33 (clone h67.6) antibodies were directly conjugated to phycoerythrin (PE) fluorophore and diluted 1:50 (working concentration of 4 μg/ml) in staining solution at 4℃ for 30 min to prevent any receptor internalisation. For detection of CD33m, mouse anti-human CD33 (clone HIM3-4) conjugated to phycoerythrin (PE) fluorophore (RRID:AB_10855031, Thermofisher Scientific) was diluted 1:50 (working concentration of 2 μg/ml) in staining solution and incubated at 4℃ for 30 min, to prevent receptor internalisation. All cells were washed with 1X PBS and FL-2 fluorescence quantified using a flow cytometer (Accuri C6, BD systems).

2.8 | Phagocytosis assays

For pH-Rodo (ThermoFisher Scientific, P36600) stained isolated synapses, neuronal debris and Alexa Fluor 555-labelled amyloid beta (Anaspec, ANA60480-01). Cells were seeded in triplicate 24 hr prior to target addition at 20,000 cells per well in DMEM supplemented with 0.5% heat-inactivated FBS and 1% penicillin/streptomycin. Preparation of monomeric, oligomeric and fibrillar amyloid beta was conducted as described previously (Neniskyte et al. 2011). Isolated synapses were prepared as described by Dunkley et al (2008). Neuronal debris were obtained by scraping cells from live neuronal–glial culture (85% neurons), cells were passed through a 0.4 × 13-mm needle 10 times, then fluorescently labelled with TAMRA (Nomura et al., 2017). For uptake into mouse BV-2 cells, we used rat neuronal debris because rat and mouse are genetically similar, and more neurons can be obtained from rats (consistent with the 3Rs). Whereas for human CHME3 cells, we made neuronal debris from human SH-SY5Y cells (RRID:CVCL_0019). SH-SY5Y cells were cultured to confluency, then harvested using trypsin and resuspended in 1X PBS. Cells were passed through 0.4 × 13-mm needle 10 times, then fluorescently labelled with TAMRA. Protein concentration of both rat and human neuronal debris was determined using Pierce BCA assay (ThermoFisher Scientific, 23227).

For uptake of fluorescent sky blue five micron carboxylated beads (Spherotech, FP-0570-2) and pH-Rodo-labelled PC12 (RRID:CVCL_0481, ECACC) cells were seeded, in duplicate, 24 hr prior to target addition at 50,000 cells per well in DMEM supplemented with 0.5% heat-inactivated FBS and 1% penicillin/streptomycin. For 0.005% w/v fluorescent sky blue five micron carboxylated beads and 300,000 live or dead pH-Rodo-labelled PC12 incubation time was 3 hr with BV-2 cells. For 16 μg of isolated synapses, 30 μg of rat neuronal debris and 2 μM of amyloid beta incubation time was 1 hr with BV-2 cells. Finally, for 60 μg of human SH-SY5Y neuronal debris, incubation time was 3 hr with CHME3 cells.

After incubation, cells were washed once with 1X PBS to remove non-phagocytosed cargo and then harvested using trypsin, pelleted and finally resuspended in 1X PBS for flow cytometry (Accuri C6, BD systems). To check the contribution of phagocytosis to apparent uptake, we inhibited phagocytosis with 10-μM cytochalasin D for 1 hr before adding phagocytic targets (Figures S3–S7).

2.9 | Sialidase treatment and assessment of desialylation

For cells treated with sialidase enzyme, 5% exogenous neuraminidase enzyme (Sigma, N3001-4UN) was added to cells for 1 hr before adding phagocytic target. To assess extent of desialylation BV-2 cells were stained with FITC-conjugated peanut agglutinin (PNA), which binds to the penultimate sugars of desialylated glycans (galactose followed by N-acetylglucosamine residues). Sialylation blocks PNA binding and therefore increased binding indicates desialylation.

2.10 | Flow cytometry

For flow cytometry, an Accuri C6 flow cytometer was used (BD systems). At least 5,000 events were analysed for each treatment replicate. FlowJo (version 10) was used for creating raw histograms and flow plots. Fc blocking antibodies were not used. Forward and side scatter was used to distinguish cells from unphagocytosed targets, i.e., beads, debris and synapses, by gating on cells in the forward and side scatter plots. Within this scatter gate, a fluorescence gate was set to identify cells that were over a threshold of fluorescence. For phagocytic targets, this fluorescence gate was set so that for cells incubated in the absence of any fluorescent targets (i.e. absence of fluorescent beads, debris, synapses, Aβ or targets cells), 99% of the cells were below this gated fluorescence and 1% were above this gate. So, for cells incubated in the presence of fluorescent targets, the % of cells with fluorescence greater than the gated fluorescence were used as the measure the % of cells that had phagocytosed the targets. For detection of GFP (green fluorescent protein), PE (phycoerythrin) and pH-rodo, a 488-nm excitation laser was used, and fluorescence emission was measured using the following channels/detectors: FL-1/FITC, FL-2/PE, FL-3/PerCP-A respectively. For detection of sky blue fluorescent beads, a 640-nm excitation laser and FL-4/APC-A detector were used. For quantification of CD33 protein on the surface of cells, forward and side scatter was used to identify cells, and the FL-2/PE fluorescence of IgG control-PE treated cells was used to gate the fluorescence of anti-CD33-PE-treated cells.

2.11 | Attachment/xCELLigence assay

For attachment assays, E-plates (ACEA biosciences, 00300600900) 96-well plates were used. First, the plate was coated with 10 μg/ml human fibronectin (Sigma, F0895) for at least 1 hr at room temperature (18°C). The plate was then blocked with 3% BSA for 1 hr at room temperature (18°C). The plate was then washed three times with 1X PBS, followed by addition of cells (15,000 per well). Real-time cell impedance measurements were collected using xCELLigence software (ACEA biosciences) for at least 4 hr.

2.12 | Migration assay

Cells were seeded at 20,000 per well in DMEM supplemented with 0.5% heat-inactivated FBS and 1% penicillin/streptomycin in the top compartment of trans-well apparatus (Coring, 3422). Cells were agitated slowly for 2 min and then allowed to settle in incubator for at least 15 min before adding treatments to the bottom compartment. Treatments were as follows: 100 μM ATP and DMEM supplemented with 0.5% heat-inactivated FBS and 1% penicillin/streptomycin. DMEM supplemented with 0.5% FBS was used as a control so there would be no concentration gradient between the top and bottom compartment of the trans-well. BV-2 cells were incubated for 2 hr, while CHME3 cells were incubated for 6 hr, both at 37°C, 5% CO_2. Cells were fixed with 4% paraformaldehyde (PFA) and stained with 4′,6-diamidino-2-phenylindole (DAPI), then imaged using an EVOS microscope system (Thermofisher). The number of cells present on the bottom of the membrane (and therefore had migrated through the trans-well) was determined by the number of DAPI-positive nuclei.

2.13 | Proliferation assays

For both BV-2 and CHME3s, cells were seeded at 100,000 per ml (final volume of 10 ml) in a T-75 flask and cultured in DMEM supplemented with 10% heat-inactivated FBS and 1% penicillin/streptomycin for 48 hr. Cells were then harvested with trypsin and counted using a haemocytometer. To ensure BV-2 cells were not proliferating during the 24-hr period between seeding and phagocytosis assays, cells were plated at 100,000 per ml in 24-well plate in DMEM supplemented with 0.5% heat-inactivated FBS and 1% penicillin/streptomycin for 24 hr. They were then harvested with trypsin and counted using a haemocytometer.

2.14 | Immunohistochemistry

For Ki-67 immunofluorescence, cells were plated at 100,000 per ml on coverslips in DMEM supplemented with 0.5% heat-inactivated FBS and 1% penicillin/streptomycin. After 24 hr, cells were washed with 1X PBS, fixed with 4% paraformaldehyde (PFA) for 15 min, permeabilised with 0.1% Triton-X:PBS for 5 min and then blocked in 3% BSA for at least 1 hr. After blocking, anti-Ki-67 antibody (RRID:AB_2142366, Millipore) was added at 1:50 dilution (working concentration of 2 μg/ml) in 3% BSA overnight at 4°C in a humidifying chamber. Then, cells were washed with 1X PBS three times, followed by incubation of secondary antibody (RRID:AB_2556776, Invitrogen) diluted 1:1,000 in 3% BSA for 1 hr at room temperature (18°C). Finally, cells were washed with 1X PBS three times, mounted on slides using mounting medium (containing 4′,6-diamidino-2-phenylindole, DAPI) (Vector Laboratories, H-1200) and imaged using epifluorescence microscope (Leica, DM16000 CS).

2.15 | Statistical analysis

The statistical analysis was performed on GraphPad prism (version 8.0) data shown represented as a mean of at least $n = 3$ independent cell cultures preparations ± *SEM*. Shapiro–Wilk test of normality was performed; however, no outlier tests were performedThe usage "Shapiro–Wilk test normality test" has been changed to "Shapiro–Wilk test of normality". Please check.. Statistical significance was assessed by repeated measures one-way ANOVA followed by Dunnett's or Tukey's *post hoc* test or paired Student's *t* test, unless stated otherwise. $p \leq .05$ were considered significant.

3 | RESULTS

3.1 | CD33M inhibits, whilst CD33m increases phagocytosis of diverse targets by BV-2 cells

We stably expressed variants of human CD33 in the mouse microglial BV-2 cells using lentivirus vectors expressing either: (1) enhanced green fluorescent protein (EGFP) as control, (2) human, full-length CD33 (CD33M), (3) human, exon 2 lacking CD33 (CD33m) or (4) the K7R variant of human, full-length CD33 (K7R-CD33M). The K7R variant cannot be ubiquitinated and thus has higher protein expression (Walter et al., 2007). We confirmed expression of the intended mRNA transcripts and CD33 protein on the plasma membrane (Figure S1 and S2). We then tested whether expression of the CD33 variants affected microglial phagocytosis of various targets: (1) carboxylated five micron beads, which mimic the size and charge of cells, (2) neuronal debris, prepared by disruption of a neuronal culture, (3) isolated synapses, prepared as synaptosomes from rat brains, (4) live PC12 cells, a neuroendocrine cell line and (5) dead PC12 cells, killed with 2-μM staurosporine. For all five phagocytic targets, there were similar trends: CD33M and K7R-CD33M expression inhibited phagocytosis, whereas CD33m expression increased phagocytosis, relative to the control transfection, although some changes were not significant (Figure 1). Representative raw flow plots can be seen in Figures S3–S7. Microglial phagocytosis expressed as the mean % of cells phagocytosing these targets ± *SEM* were for beads: control 30 ± 3, CD33M 26 ± 2, CD33m 36 ± 4, K7R-CD33M 23 ± 3,

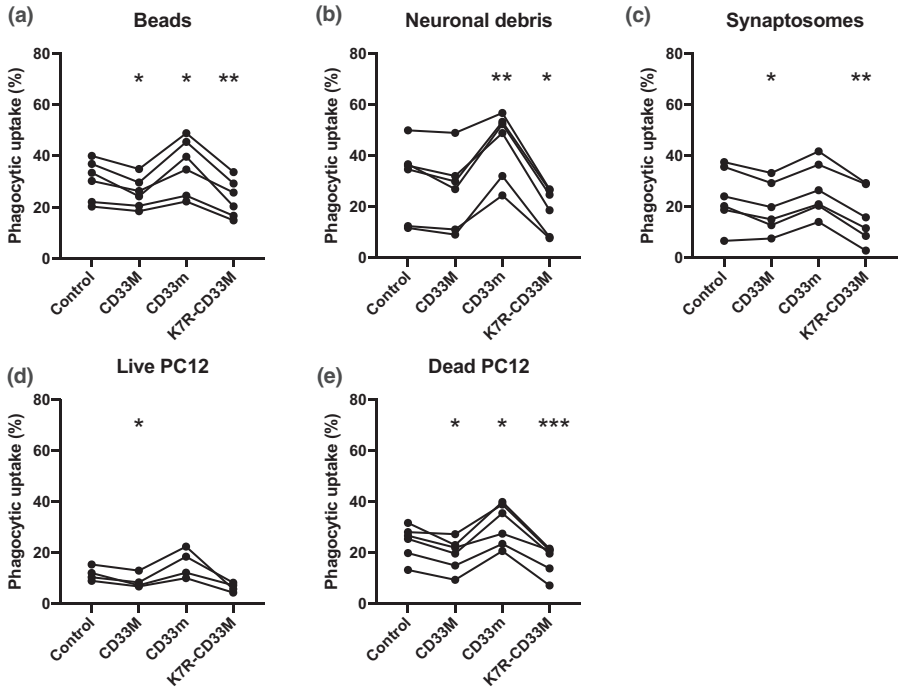

FIGURE 1 CD33M decreases and CD33m increases microglial phagocytosis of beads, debris, synapses and cells. Phagocytosis by CD33M/m-expressing BV-2 cell lines of: (a) carboxylated beads, (b) neuronal debris, (c) isolated synapses, (d) live PC12 cells and (e) dead PC12 cells. For all experiments, $n = 4–6$ independent cell culture preparations. Repeats done on the same day with the four variant cell lines are linked by solid lines. Statistics: repeated measures one-way ANOVA, * is with respect to control, *p <.05, **p <.01, ***p <.001

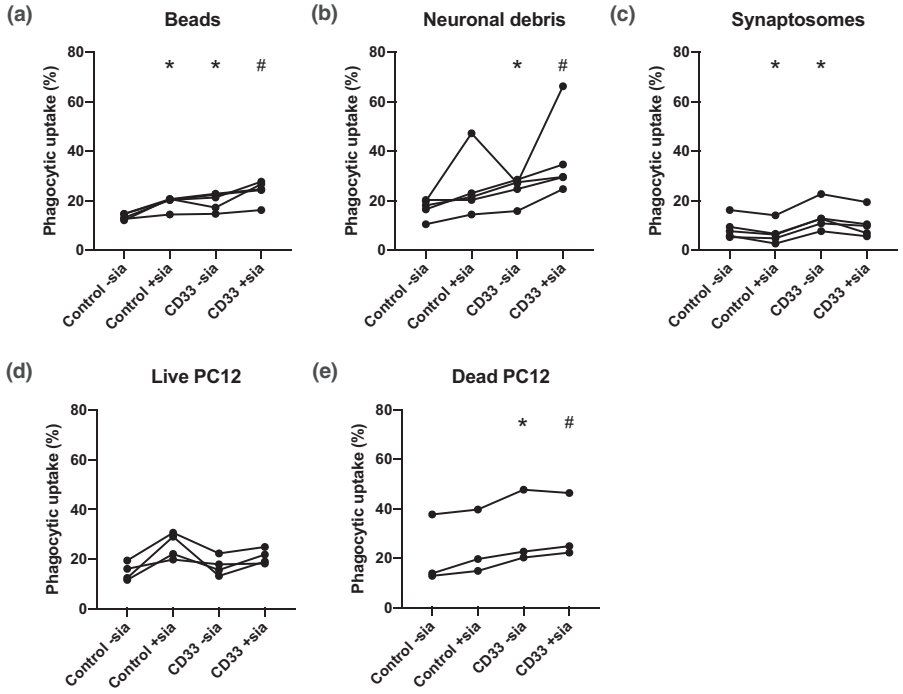

FIGURE 2 Knockdown of mouse CD33 and/or sialidase increases microglial phagocytosis. Phagocytosis by BV-2 cells treated ± sialidase with non-targeting control RNAi or CD33 RNAi of: (a) five micron beads, (b) neuronal debris, (c) isolated synapses and (d) live PC12 cells. For all experiments $n = 3–5$ independent cell culture preparations. Repeats done on the same day with the four variant cell lines are linked by solid lines. Statistics: repeated measures one-way ANOVA, * is with respect to control -sialidase, # is with respect to control + sialidase. */# p <.05

(Figure 1a), for neuronal debris: control 30 ± 6, CD33M 26 ± 6, CD33m 4.5 ± 4, K7R-CD33M 19 ± 4 (Figure 1b), for isolated synapses: control 24 ± 5, CD33M 20 ± 4, CD33m 27 ± 4, K7R-CD33M 16 ± 4 (Figure 1c), for live PC12 cells: control 12 ± 1, CD33M 9 ± 1, CD33m 16 ± 3, K7R-CD33M 6 ± 1 (Figure 1d) and for dead PC12 cells: control 24 ± 3, CD33M 19 ± 3, CD33m 31 ± 3, K7R-CD33M 17 ± 2 (Figure 1e). Thus, CD33M inhibits phagocytosis and CD33m increases phagocytosis.

3.2 | Knockdown of endogenous mouse CD33 or desialylation of cells increases phagocytosis by BV-2 cells

As expression of human CD33M in mouse BV-2 cells inhibited phagocytosis, we tested whether knockdown of the endogenous mouse CD33 would increase phagocytosis, as the role of mouse CD33 remains unclear. We confirmed that the RNAi directed to mouse CD33 reduced CD33 protein expression at the plasma membrane by 50%–60% (Figure S8b & c). RNAi knockdown of endogenous mouse CD33 increased microglial phagocytosis of all targets. Results are expressed as mean % of cells phagocytosing targets ± *SEM*: beads (control RNAi 13 ± 1, CD33 RNAi 20 ± 2, Figure 2a), neuronal debris (control RNAi, 17 ± 2, CD33 RNAi 25 ± 2, Figure 2b), synapses (control RNAi 9 ± 2, CD33 RNAi 13 ± 2, Figure 2c), live PC12 cells (control RNAi 15 ± 2, CD33 RNAi 17 ± 2, Figure 2d) and dead PC12 cells (control RNAi 21 ± 8, CD33 RNAi 30 ± 9, Figure 2e). Note that CD33 knockdown and desialylation did not significantly affect uptake of live cells. These data indicate that endogenous mouse CD33 inhibits microglial phagocytosis similarly to human CD33M.

Because CD33 is a sialic acid-binding receptor potentially regulated by sialylation of the cell surface (Brinkman-Van der Linden et al., 2003), we tested whether desialylation of the cells affected phagocytosis via CD33. We desialylated the microglia by pre-incubation with sialidase for 1 hr, and verified effective desialylation by assaying the binding of peanut agglutinin (PNA), which binds galactose residues only after the removal of terminal sialic acid residues that block PNA binding (Figure S8d). Desialylation of the microglia increased phagocytosis of beads. All results are expressed as mean % of cells phagocytosing targets ± *SEM*: control no sialidase 13 ± 1, after sialidase treatment to 19 ± 1 (Figure 2a), but decreased phagocytosis of synapses: control no sialidase 9 ± 2, after sialidase treatment 7 ± 2 (Figure 2c). Desialylation also increased phagocytosis of neuronal debris and cells, but these changes were not significant (Figure 2b, d & e). Knockdown of mouse CD33 prevented the effect of desialylation on phagocytosis of beads (CD33 no sialidase 20 ± 2, after sialidase treatment to 24 ± 2, Figure 2a) and synapses (CD33 no sialidase 13 ± 3, after sialidase treatment 10 ± 2, Figure 2c). This suggests that the effect of desialylation on phagocytosis could be partly mediated via CD33. However, desialylation still increased phagocytosis of beads and decreased phagocytosis of synapses after CD33 knockdown, so desialylation appears to increase phagocytosis at least partly by CD33-independent means.

3.3 | Knockdown of endogenous mouse CD33 prevents human CD33m increasing phagocytosis in BV-2 cells

One possible means by which human CD33m expression might increase phagocytosis is by disrupting the function of endogenous mouse CD33 (e.g. by dimerising with it). To test this possibility, we compared the effect of human CD33 expression on phagocytosis in the presence or absence of endogenous mouse CD33 knockdown using RNAi. We chose to examine the effect of knockdown and expression on phagocytosis of neuronal debris as this may be the most physiological relevant target of phagocytosis, and had a robust response to CD33 expression (Figure 1b). As expected, in BV-2 cells treated with a control, non-targeting RNAi, CD33M and K7R-CD33M reduced phagocytosis, and CD33m increased phagocytosis. Phagocytosis is expressed as mean % of cells phagocytosing debris ± *SEM* were: control 12 ± 2, CD33M 8 ± 1, CD33m 18 ± 2, K7R-CD33M 6 ± 1 (Figure 3a). However, in cells treated with RNAi to knockdown endogenous mouse CD33, CD33m did not change phagocytosis, while CD33M and K7R-CD33M still reduced phagocytosis: control 28 ± 5, CD33M 18 ± 3, CD33m 29 ± 5, K7R-CD33M 11 ± 1 (Figure 3b). This is consistent with human CD33m increasing phagocytosis by disrupting the function of endogenous mouse CD33.

3.4 | CD33m increases monomeric Aβ uptake, and CD33M inhibits fibrillar Aβ uptake by BV-2 cells

CD33M has previously been shown to inhibit microglial uptake of Aβ, but the form of Aβ was undefined (Bradshaw et al., 2013; Griciuc et al., 2013). So, we tested the effect of the various human CD33

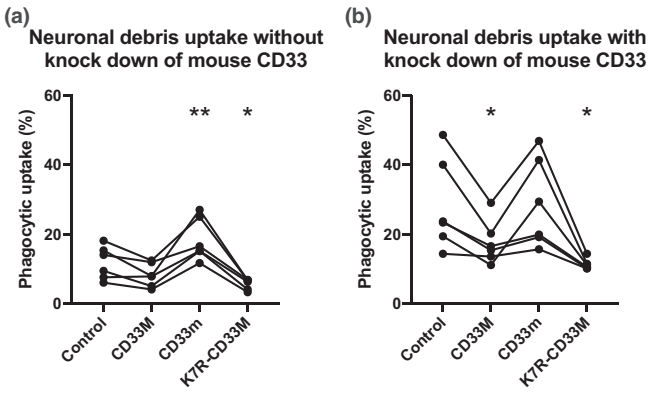

FIGURE 3 Knockdown of endogenous mouse CD33 prevents human CD33m increasing phagocytosis. (a) BV-2 cells expressing human CD33 variants were subjected to either control/scrambled RNAi or (b) mouse CD33 targeting RNAi and percentage of phagocytosis of rat neuronal debris was quantified using flow cytometry. $N = 6$ independent cell culture preparations. Repeats done on the same day with the four variant cell lines are linked by solid lines. Statistics: repeated measures, one-way ANOVA. * is with respect to control (a) scrambled RNAi or (b) CD33 RNAi treated) *$p < .05$, **$p < .01$

variants on microglial uptake of monomeric, oligomeric and fibrillar A. CD33M and K7R-CD33M had a tendency to inhibit uptake of all forms of Aβ; however, only the inhibition of monomeric Aβ uptake by CD33M was statistically significant (Figure 4). CD33m had a tendency to increase uptake of all forms of Aβ; however, only the increased uptake of monomeric Aβ by CD33m was statistically significant (Figure 4). Results are expressed as mean % of cells phagocytosing Aβ ± *SEM*. For monomeric Aβ: control 23 ± 8, CD33M 21 ± 8, CD33m 28 ± 9, K7R-CD33M 12 ± 4 (Figure 4a), for oligomeric Aβ: control 16 ± 5, CD33M 14 ± 5, CD33m 22 ± 7, K7R-CD33M 9 ± 4 (Figure 4b) and for fibrillar Aβ: control 55 ± 12, CD33M 48 ± 12, CD33m 65 ± 10, K7R-CD33M 32 ± 12 (Figure 4c). Thus, there is a tendency for CD33M to decrease Aβ uptake, and for CD33m to increase Aβ uptake, as seen with phagocytosis of all other phagocytic targets (Figure 1).

3.5 | K7R-CD33M increases cell attachment to fibronectin, whilst CD33m decreases attachment to fibronectin in BV-2 cells

Microglial migration is in part determined by cellular adhesion to extracellular matrix, so we tested whether the CD33 variants affected microglial adhesion to fibronectin (which is a major component of brain extracellular matrix) measured by the increase in impedance as the cells adhere and spread on fibronectin-coated plates. K7R-CD33M increased adhesion to fibronectin (K7R-CD33M 194 ± 27% of control ± *SEM*, Figure 5), while CD33m reduced adhesion (CD33m 51 ± 9% of control ± *SEM*, Figure 5). CD33m reduced cell spreading on the same matrix measured as the area of the plates occupied by the cells (Figure S9). Thus, CD33M over-expression appears to increase matrix adhesion and CD33m reduces matrix adhesion.

3.6 | CD33M inhibits migration of BV-2 cells towards ATP

Phagocytosis of targets normally requires migration to those targets, so we tested whether the CD33 variants affected microglial migration through a trans-well in response to a chemotactic gradient of ATP. ATP increased migration through the trans-well by control and CD33m-expressing microglia. Results expressed as cell numbers migrated ± *SEM*. (ATP control: 1,095 ± 179, ATP + CD33m: 905 ± 135, Figure 6a), but did not significantly stimulate migration of cells expressing CD33M or K7R-CD33M (ATP + CD33M 568 ± 112, ATP + K7R-CD33M: 598 ± 133, Figure 6a). This indicates that CD33M inhibits microglial migration to ATP.

3.7 | CD33M reduces microglia proliferation, whilst CD33m increases proliferation in BV-2 cells

Because cellular adhesion to substrate can affect proliferation (Lundell et al., 1996; Schwartz & Assoian, 2001), we tested whether the CD33 variants affected microglial proliferation, measured as cell numbers after 48 hr in 10% serum. CD33M and K7R-CD33M inhibited proliferation, while CD33m increased cell proliferation. Results expressed as cell numbers per mL ± *SEM* were: for control 813 ± 68, K7R-CD33M 513 ± 59, CD33M 607 ± 84, CD33m 920 ± 61 (Figure 6b). Similarly, CD33M and K7R-CD33M inhibited cellular Ki-67 immunostaining (a marker of cell proliferation), while CD33m increased Ki-67 staining (Figure S10a).

Because the CD33 variants affected cell proliferation measured as cell numbers after 48 hr in 10% serum, we checked whether the CD33 variants affected cell numbers in the conditions used to assay phagocytosis by plating BV-2 cells in DMEM supplemented with 0.5% serum and counting cell numbers after 24 hr. We saw no differences in cell numbers between the different lines in these conditions (Figure S10b), indicating that any apparent differences in phagocytosis between the variants were not owing to differences in cell number.

3.8 | CD33M decreases phagocytosis and proliferation but increases adhesion to fibronectin in human CHME3 cells

To test whether the effects of expressing human CD33 variants in mouse BV-2 cells were also seen in human cells, we stably

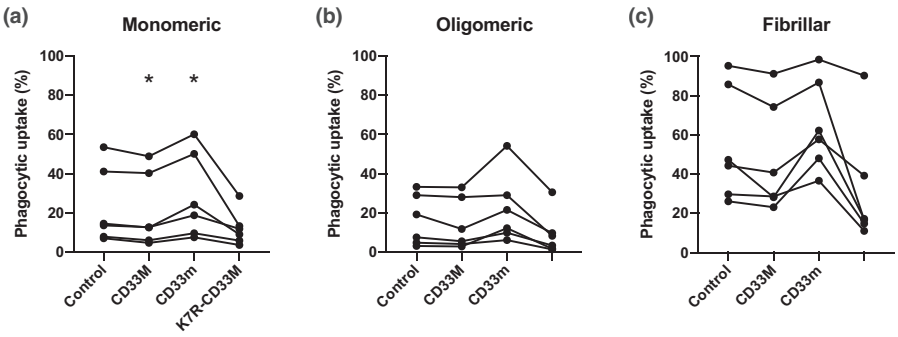

FIGURE 4 K7R-CD33M inhibits microglial phagocytosis of Aβ. Phagocytosis by CD33M/m-expressing BV-2 cells of: (a) monomeric Aβ, (b) oligomeric Aβ or (c) fibrillar Aβ. For all experiments $n = 6$ independent cell culture preparations. Repeats done on the same day with the four variant cell lines are linked by solid lines. Statistics: repeated measures one-way ANOVA, * is with respect to the control cells, *p <.05

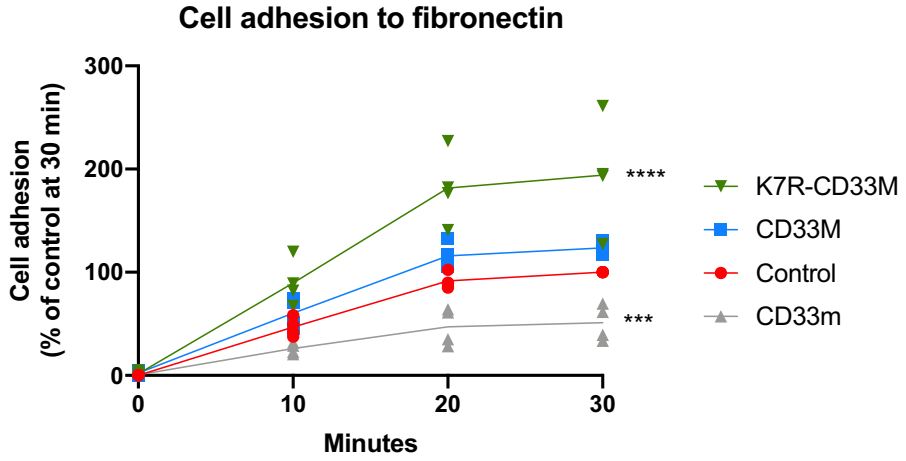

FIGURE 5 K7R-CD33M increases and CD33m decreases cell attachment to fibronectin. Attachment of human CD33 variant-expressing BV-2 cells to fibronectin over 30 min, measured by electrical impedance of cell layer. $n = 4$ independent cell culture preparations. Statistics: two-way ANOVA. * is with respect to control cells. ***$p < .001$, ****$p < .0001$

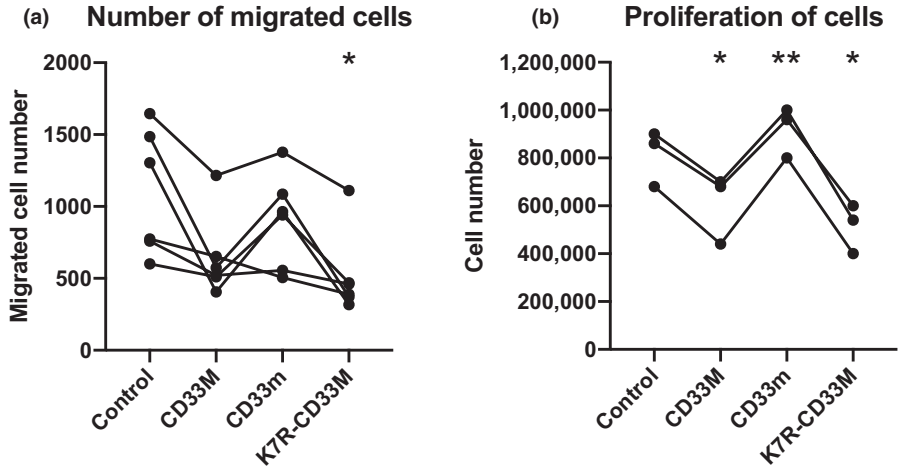

FIGURE 6 CD33M decreases migration and cell proliferation, whereas CD33m increases cell proliferation. (a) Number of DAPI-positive nuclei (of ATP-induced migrated cells) present on bottom of trans-well membrane following 2-hr incubation. $N = 6$ independent cell culture preparations. Statistics: repeated measures one-way ANOVA. (b) Proliferation rate was measured as cell density (counted by haemocytometer) 48 hr after seeding the same density of cells in DMEM supplemented with 10% heat-inactivated FBS. $N = 3$ independent cell culture preparations. Repeats done on the same day with the four variant cell lines are linked by solid lines. Statistics: repeated measures one-way ANOVA, * is with respect to control, *$p < .05$, **$p < .01$

expressed the same human CD33 variants in a human microglia cell line, CHME3 cells. CHME3 cells were derived by SV40-dependent immortalisation of human embryonic microglial cells, and are also known as HMC3 cells (Dello Russo et al., 2018).

We confirmed expression of the CD33 variants at the level of both mRNA and cell surface protein CHME3 after lentiviral transfection of the CHME3 cells (Figure S11 & S12).

To assess the effect of the isoforms on phagocytosis, we tested uptake of pH-rodo-labelled neuronal debris from human SH-SY5Y neuroblastoma cells. We found that expression of CD33M and K7R-CD33M inhibited phagocytosis, while CD33m increased phagocytosis of debris compared to control. Results expressed as mean % of cells phagocytosing debris ± *SEM* (control 22 ± 4, CD33M 17 ± 3, CD33m 35 ± 3, K7R-CD33M 9 ± 2, Figure 7a). These findings are consistent with those seen in the BV-2 cells (Figures 1b & 3a), i.e., CD33M increases phagocytosis, while CD33m decreases phagocytosis.

We assessed proliferation of CHME3 cells expressing the different CD33 variants by seeding the same cell numbers then counting cells 48 hr later. We found that expression of CD33M and K7R-CD33M decreased the proliferation rate, whereas expression of CD33m increased the proliferation rate compared to the control cells. Results expressed as cell number per mL ± *SEM* (control 290 ± 12, CD33M 225 ± 10, K7R-CD33M 140 ± 12, CD33m 405 ± 17, Figure 7b). Again, these data are consistent with the findings seen in the BV-2 cells (Figure 6b). Note that CHME3 cells proliferate at a slower rate than BV-2 cells, and therefore the cell numbers were lower, but the same effect of CD33M decreasing

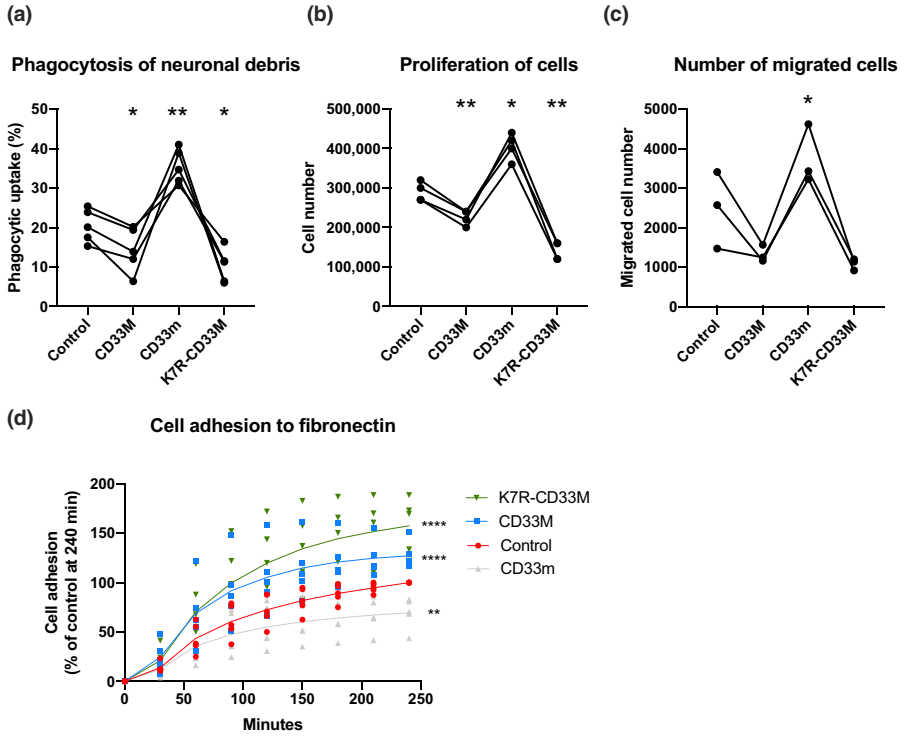

FIGURE 7 In human CHME3 cells, CD33M decreases and CD33m increases microglial phagocytosis, migration and proliferation, but CD33M increases adhesion whereas CD33m decreases adhesion. (a) Phagocytosis of 60 μg of human SH-SY5Y neuronal debris by CHME3 cells expressing CD33 variants. $n = 5$ independent cell culture preparations. Statistics: repeated measures one-way ANOVA. * is with respect to control cells, *p <.05, **p <.01. (b) Proliferation rate was measured as cell density (counted by haemocytometer) 48 hr after seeding the same density of cells in DMEM supplemented with 10% heat-inactivated FBS. $N = 4$ independent cell culture preparations. Statistics: repeated measures one-way ANOVA. * is with respect to control cells, *p <.05, **p <.01. (c) Migration was measured as the number of DAPI-positive cells present on bottom of the trans-well, 6 hr after adding cells above the trans-well and adding ATP below the trans-well. $N = 3$ independent cell culture preparations. Repeats done on the same day with the four variant cell lines are linked by solid lines. Statistics: repeated measures one-way ANOVA, * is with respect to CD33M cells, *p <.05. (d) Attachment of human CD33 variant-expressing CHME3 cells to fibronectin over 240 min, measured by electrical impedance of cell layer. Statistics: two-way ANOVA. * is with respect to control cells, **p <.01, ****p <.0001

proliferation and CD33m increasing proliferation was found in the two cell lines.

To assess migration of CHME3 cells expressing the CD33 variants, we counted cells migrating through a trans-well in response to an ATP gradient, as previously for BV-2 cells. CD33M had a tendency to decrease migration, and CD33m had a tendency to increase migration, but due to the variability of the control, the only significant difference was between CD33M and CD33m. Results expressed as mean % of migrated cells ± *SEM* were: control 2,485 ± 560, CD33M 1,326 ± 123, CD33m 3,759 ± 434 and K7R-CD33M 1,086 ± 87 (Figure 7c). These findings are consistent with those seen in BV-2 cells (Figure 6a), i.e. CD33m has the opposite effect to CD33M on migration.

Finally, to assess the effect of CD33 variants on cellular adhesion, we measured the rate of adhesion to fibronectin-coated plates as before, but for a longer period of time (4 hr), as CHME3 cells took longer to adhere to surfaces than BV-2 cells. Expression of CD33M and K7R-CD33M increased adhesion, whereas CD33m decreased adhesion. Results expressed as % of control at 4 hr ± *SEM* (control 62 ± 12, CD33M 87 ± 15, K7R-CD33M 100 ± 19, Figure 7d). These results in CHME3 cells are consistent with the findings in BV-2 cells (Figure 5), i.e., CD33M increases adhesion, while CD33m decreases adhesion. Overall, the effects of expressing CD33 variants in human CHME3 cells are similar to expressing the variants in mouse BV-2 cells.

4 | DISCUSSION

CD33 is an inhibitory receptor expressed on myeloid cells, including microglia, potentially activated by sialic acid residues (Lajaunias et al., 2005). CD33m is thought to have a reduced function relative to CD33M, because of this splice variant lacking the sialic acid-binding domain (Griciuc et al., 2013; Siddiqui et al., 2017). Consistent with this, it was reported that CD33M inhibited microglial phagocytosis of Aβ, while CD33m had no effect. This could explain why expression of CD33m, rather than CD33M, apparently protects against AD, as it has lost the capacity to inhibit microglia phagocytosis (Griciuc et al., 2013; Siddiqui et al., 2017). However, we show that expression of CD33m actually increases microglial phagocytosis of multiple

phagocytic targets (beads, debris and cells) compared to control. While expression of CD33M had the opposite effect, decreasing the phagocytosis of these targets, as well as synapses.

Estus et al., (2019) argued that CD33m may have a gain of function, because another CD33 variant that is effectively a knockout does not decrease risk of AD. A potential mechanism for such a gain of function could be that CD33m heterodimerises with CD33M to block its function potentially via the C2 domains of both isoforms (Estus et al., 2019). We find that expression of CD33m in the BV-2 cells increases microglial phagocytosis, but this effect is lost when endogenous mouse CD33 is knocked down, which itself increases phagocytosis. This suggests that human CD33m may have a dominant negative effect over mouse CD33M, potentially by heterodimerising with it. However, CD33m also had the opposite effects to CD33M in human CHME3 that do not express endogenous CD33 (Figures S11 and S12). Siddiqui et al. (2017) found endogenous expression of CD33M and CD33m in CHME5 cells, but it remains unclear how these cells are related to CHME3 cells (Dello Russo et al., 2018). As CD33m expression affected CHME3 functions in the absence of CD33M, CD33m may also have effects independent of CD33M. Possibilities might include: CD33m acting as an ITAM receptor (Estus et al., 2019), CD33m acting intracellularly (Siddiqui et al., 2017) or CD33m binding SHP-1/2 without activating them and thereby inhibiting their activation. As we see a small proportion of CD33m present on the cell surface but a large expression of CD33m mRNA in both BV-2 and CHME3 cells (Figures S1, S2, S11 and S12), it is feasible that CD33m is more highly expressed intracellularly, although we have not tested this.

It could be argued that the various phagocytic targets we have used, including Aβ, beads, neuronal debris, isolated synapses and dead cells, are all forms of "debris". It is generally thought that extracellular debris accumulates in the brain with neurodegenerative diseases (Takahashi et al., 2007; Neumann et al., 2008; Marquez-Ropero et al. 2020). Neurodegeneration may generate debris as dead neurons and bits of neurons, but such debris might also induce neurodegeneration, for example, by activating microglia (Map his et al., 2015; Spangenberg et al., 2016). Thus, one possible means by which CD33M may predispose to AD is by blocking microglial phagocytosis of the debris accumulating during neurodegeneration (or ageing), thereby exacerbating neuroinflammation.

TREM2 is one of the main phagocytic receptors mediating microglial phagocytosis of debris (Takahashi et al., 2005), and loss-of-function mutations in TREM2 predispose to AD (Sudom et al., 2018), and this might potentially be due to reduced microglial phagocytosis of debris. CD33 could potentially antagonise phagocytic signalling by TREM2 (or CR3), as TREM2 and CR3 activate phagocytosis via inducing phosphorylation of the tyrosine-protein kinase Syk, while CD33 activates the tyrosine-protein phosphatases SHP-1 and SHP-2 (Paul et al., 2000), which may dephosphorylate Syk and Syk substrates. This may be one potential mechanism by which CD33M is inhibiting phagocytosis in our study. Consistent with this, Griciuc et al. (2019) showed that in the 5XFAD mouse model of AD, TREM2 knockout increased the pathology, while CD33 knockout reduced the pathology, but knocking out both TREM2 and CD33 resulted in the increased pathology of the TREM2 knockout, suggesting that TREM2 was acting "downstream" of CD33 to induce these effects. These results are consistent with CD33 simply suppressing TREM2 signalling via activating SHP-1/2 (as CD33 then requires TREM2 signalling to have an effect), but they do not rule out more complex interactions between CD33 and TREM2.

Mouse and human CD33 have homologous extracellular domains, and divergent intracellular domains, but whether their functions diverge is less clear. Bhattacherjee et al., (2019) found that expression of human CD33 inhibited phagocytosis, but expression of mouse CD33 did not inhibit phagocytosis (Bhattacherjee et al., 2019). However, Gricuic et al., (2013) found that knockout of CD33 increased microglial phagocytosis of amyloid beta, and this is consistent with our finding that RNAi knockdown of mouse CD33 increased phagocytosis of beads, debris and synapses. These discrepancies between groups could be because of different experimental techniques, cells, animals, levels of CD33 expression or levels of cell sialylation.

CD33 is thought to be an inhibitory receptor potentially activated by sialic acid residues of other glycoproteins (Lajaunias et al., 2005). We find that desialylation of microglia by adding sialidase increases phagocytosis of beads, consistent with previous findings (Allendorf et al., 2020; Nomura et al., 2017; Pluvinage et al., 2019), but decreased phagocytosis of synapses. RNAi knockdown of mouse CD33 reduced the effect of desialylation on phagocytosis, suggesting that CD33 may contribute to this effect, but the data were not robust enough to make a firm conclusion. Recently, Pluvinage et al., (2019) showed that CD22 (Siglec-2) was required for the effect of sialylation/desialylation on microglial phagocytosis (Pluvinage et al., 2019); and Allendorf et al. (2020) found that complement receptor 3 was also required (Allendorf et al., 2020). As different phagocytic receptors may be required for phagocytosis of beads and synapses, it seems reasonable that desialylation may affect these different receptors differently, resulting in increased phagocytosis of beads but decreased phagocytosis of synapses.

Microglial phagocytosis normally requires microglial migration, so we tested the effect of CD33 on migration of microglia through trans-wells in response to a chemotactic gradient of ATP. We found that expression of human CD33M in both cell types inhibited microglial migration towards ATP, whereas expression of CD33m did not inhibit migration. CD33M also increased microglial attachment to fibronectin in CHME3 cells but only with supraphysiological levels of CD33M (K7R-CD33M) in BV-2 cells. Whereas CD33m reduced both attachment to fibronectin in both cell lines and cell spreading on fibronectin in the BV-2 cells. Together, these findings suggest that over-expression of CD33M increases microglial attachment, which may reduce migration, and potentially reduce phagocytosis. Whereas CD33m decreases attachment, potentially causing increased phagocytosis.

Increased adhesion has been linked to reduced migration in a number of cell types (DiMilla et al., 1991; Palecek et al., 1997; Schmidt & Friedl, 2010). Thus, it is possible that the increase in adhesion

induced by CD33M might contribute to reduced migration found in the presence of ATP. Other Siglecs have been shown to inhibit migration, including Siglec-E in inhibition of neutrophil and monocyte recruitment, and CD22 in inhibition of B cell migration and adhesion (McMillan et al., 2013; Nitschke et al., 1997). CD33 has been shown to mediate adhesion of CD33-expressing cells to erythrocytes via binding to sialic acid residues on the erythrocytes (Freeman et al., 1995). It could be that over-expression of CD33M increases cellular adhesion and spreading by binding sialic acid residues on fibronectin, but we do not think this is the case, as sialidase treatment of the fibronectin to remove sialic acid residues did not significantly decrease CD33M-induced adhesion in BV-2 cells (data not shown).

Another feature of microglial activation is proliferation: microglia can proliferate in response to damage, pathogens or inflammation. We found that CD33M inhibits proliferation, whereas CD33m stimulates proliferation in both cell lines. Increased proliferation in the presence of CD33m potentially means more microglia are present to clear debris and Aβ, and thereby potentially protecting the brain in AD. Cellular attachment can induce proliferation in some cell types (Pugacheva et al., 2006). A potential role of CD33 in proliferation has been shown as activation of CD33 by anti-CD33 antibodies reduced proliferation of leukaemic cells (Balaian et al., 2003; Vitale et al., 1999).

The microglial processes investigated in this study, proliferation, migration and phagocytosis, are all key aspects of microglia activation, and all are inhibited by CD33M. Microglia activation is a hallmark of neurodegenerative diseases such as AD. Our findings suggest a potential novel role of CD33m in increasing microglial proliferation, movement and phagocytosis of debris and Aβ, which might contribute to protecting the AD brain. However, further work is required to determine the molecular mechanisms by which CD33m and CD33M confer these differential effects on microglia.

ACKNOWLEDGEMENTS

We thank David Allendorf for help with lentiviral transfection and Dr Samir Hamara for help with xCELLigence machine. We also thank Dr Roland Walter for providing the CD33 lentiviral plasmids as a gift. CAB received funding from AstraZeneca and the Biotechnology and Biological Sciences Research Council UK. GCB received funding from the Innovative Medicines Initiative 2 Joint Undertaking under grant agreement No 115976 (PHAGO consortium) and from the Medical Research Council UK (No. MR/L010593). The authors declare that they have no competing interests. We gratefully acknowledge the financial support from AstraZeneca.

ORCID

Claire Ann Butler https://orcid.org/0000-0001-9320-8297
Guy Charles Brown https://orcid.org/0000-0002-3610-1730

REFERENCES

Allendorf, D. H., Puigdellívol, M., & Brown, G. C. (2020). Activated microglia desialylate their surface, stimulating complement receptor 3-mediated phagocytosis of neurons. *Glia*, *68*(5), 989–998.

Balaian, L., Zhong, R. K., & Ball, E. D. (2003). The inhibitory effect of anti-CD33 monoclonal antibodies on AML cell growth correlates with Syk and/or ZAP-70 expression. *Experimental Hematology*, *31*(5), 363–371. https://doi.org/10.1016/S0301-472X(03)00044-4

Bhattacherjee, A., Rodrigues, E., Jung, J., Luzentales-Simpson, M., Enterina, J. R., Galleguillos, D., St. Laurent, C. D., Nakhaei-Nejad, M., Fuchsberger, F. F., Streith, L., Wang, Q., Kawasaki, N., Duan, S., Bains, A., Paulson, J. C., Rademacher, C., Giuliani, F., Sipione, S., & Macauley, M. S. (2019). Repression of phagocytosis by human CD33 is not conserved with mouse CD33. *Communications Biology*, *3*(1), 1–13. https://doi.org/10.1038/s42003-019-0698-6

Bradshaw, E., Chibnik, L., Keenan, B., Ottoboni, L., Raj, T., Tang, A., Rosenkrantz, L., Imboywa, S., Lee, M., Von Korff, A., Morris, M., Evans, D., Johnson, K., Sperling, R., Schneider, J., Bennett, D., & De Jager, P. (2013). CD33 Alzheimer's disease locus: Altered monocyte function and amyloid biology. *Nature Neuroscience*, *16*(7), 848–850. https://doi.org/10.1038/nn.3435

Brinkman-Van der Linden, E., Angata, T., Reynolds, S., Powell, L., Hedrick, S., & Varki, A. (2003). CD33/Siglec-3 binding specificity, expression pattern, and consequences of gene deletion in mice. *Molecular and Cellular Biology*, *23*(12), 4199–4206. https://doi.org/10.1128/MCB.23.12.4199-4206.2003

Crocker, P. R., & Varki, A. (2001). Siglecs, sialic acids and innate immunity. *Trends in Immunology*, *22*, 337–342. https://doi.org/10.1016/s1471-4906(01)01930-5

Dello Russo, C., Cappoli, N., Coletta, I., Mezzogori, D., Paciello, F., Pozzoli, G., Navarra, P., & Battaglia, A. (2018). The human microglial HMC3 cell line: Where do we stand? A systematic literature review. *Journal of Neuroinflammation*, *15*, 259. https://doi.org/10.1186/s12974-018-1288-0

DiMilla, P. A., Barbee, K., & Lauffenburger, D. A. (1991). Mathematical model for the effects of adhesion and mechanics on cell migration speed. *Biophysical Journal*, *60*(1), 15–37.

Estus, S., Shaw, B., Devanney, N., Katsumata, Y., Press, E., & Fardo, D. (2019). Evaluation of CD33 as a genetic risk factor for Alzheimer's disease. *Acta Neuropathologica*, *138*(2), 187–199. https://doi.org/10.1007/s00401-019-02000-4

Freeman, S., Kelm, S., Barber, E., & Crocker, P. (1995). Characterization of CD33 as a new member of the sialoadhesin family of cellular interaction molecules. *Blood*, *85*(8), 2005–2012. https://doi.org/10.1182/blood.V85.8.2005.bloodjournal8582005

Galloway, D., Phillips, A., Owen, D., & Moore, C. (2019). Phagocytosis in the brain: Homeostasis and disease. *Frontiers in Immunology*, *10*, 790. https://doi.org/10.3389/fimmu.2019.00790

Griciuc, A., Patel, S., Federico, A., Choi, S., Innes, B., Oram, M., Cereghetti, G., McGinty, D., Anselmo, A., Sadreyev, R., Hickman, S., El Khoury, J., Colonna, M., & Tanzi, R. (2019). TREM2 acts downstream of CD33 in modulating microglial pathology in Alzheimer's disease. *Neuron*, *103*(5), 820–835. https://doi.org/10.1016/j.neuron.2019.06.010

Griciuc, A., Serrano-Pozo, A., Parrado, A., Lesinski, A., Asselin, C., Mullin, K., Hooli, B., Choi, S., Hyman, B., & Tanzi, R. (2013). Alzheimer's disease risk gene CD33 inhibits microglial uptake of amyloid beta. *Neuron*, *78*(4), 631–643. https://doi.org/10.1016/j.neuron.2013.04.014

Hernández-Caselles, T., Martínez-Esparza, M., Pérez-Oliva, A., Quintanilla-Cecconi, A., García-Alonso, A., Alvarez-López, D., & García-Peñarrubia, P. (2006). A study of CD33 (SIGLEC-3) antigen expression and function on activated human T and NK cells: Two isoforms of CD33 are generated by alternative splicing. *Journal of Leukocyte Biology*, *79*(1), 46–58. https://doi.org/10.1189/jlb.0205096

Hollingworth, P., Harold, D., Sims, R., Gerrish, A., Lambert, J., Carrasquillo, M., Abraham, R., Hamshere, M., Pahwa, J., Moskvina, V., Dowzell, K., Jones, N., Stretton, A., Thomas, C., Richards, A., Ivanov, D., Widdowson, C., Chapman, J., Lovestone, S., … Williams, J. (2011). Common variants at ABCA7, MS4A6A/MS4A4E, EPHA1, CD33 and

CD2AP are associated with Alzheimer's disease. *Nature Genetics*, *43*(5), 429–435. https://doi.org/10.1038/ng.803

Lajaunias, F., Dayer, J., & Chizzolini, C. (2005). Constitutive repressor activity of CD33 on human monocytes requires sialic acid recognition and phosphoinositide 3-kinase-mediated intracellular signaling. *European Journal of Immunology*, *35*(1), 243–251. https://doi.org/10.1002/eji.200425273

Lundell, B. I., McCarthy, J. B., Kovach, N. L., & Verfaillie, C. M. (1996). Activation-dependent alpha5beta1 integrin-mediated adhesion to fibronectin decreases proliferation of chronic myelogenous leukemia progenitors and K562 cells. *Blood*, *87*(6), 2450–2458. https://doi.org/10.1182/blood.V87.6.2450.bloodjournal8762450

Malik, M., Simpson, J., Parikh, I., Wilfred, B., Fardo, D., Nelson, P., & Estus, S. (2013). CD33 Alzheimer's risk-altering polymorphism, CD33 expression, and exon 2 splicing. *Journal of Neuroscience*, *33*(33), 13320–13325. https://doi.org/10.1523/JNEUROSCI.1224-13.2013

Maphis, N., Xu, G., Kokiko-Cochran, O., Jiang, S., Cardona, A., Ransohoff, R., Lamb, B., & Bhaskar, K. (2015). Reactive microglia drive tau pathology and contribute to the spreading of pathological tau in the brain. *Brain*, *138*(6), 1738–1755. https://doi.org/10.1093/brain/awv081

Márquez-Ropero, M., Benito, E., Plaza-Zabala, A., & Sierra, A. (2020). Microglial corpse clearance: Lessons from macrophages. *Frontiers in Immunology*, *11*, 506.

McMillan, S., Sharma, R., McKenzie, E., Richards, H., Zhang, J., Prescott, A., & Crocker, P. (2013). Siglec-E is a negative regulator of acute pulmonary neutrophil inflammation and suppresses CD11b β2-integrin–dependent signaling. *Blood*, *121*(11), 2084–2094. https://doi.org/10.1182/blood-2012-08-449983

Naj, A., Jun, G., Beecham, G., Wang, L., Vardarajan, B., Buros, J., Gallins, P., Buxbaum, J., Jarvik, G., Crane, P., Larson, E., Bird, T., Boeve, B., Graff-Radford, N., De Jager, P., Evans, D., Schneider, J., Carrasquillo, M., Ertekin-Taner, N., … Schellenberg, G. (2011). Common variants at MS4A4/MS4A6E, CD2AP, CD33 and EPHA1 are associated with late-onset Alzheimer's disease. *Nature Genetics*, *43*(5), 436–441. https://doi.org/10.1038/ng.801

Neumann, H., Kotter, M. R., & Franklin, R. J. M. (2008). Debris clearance by microglia: An essential link between degeneration and regeneration. *Brain*, *132*(2), 288–295. https://doi.org/10.1093/brain/awn109

Nitschke, L., Carsetti, R., Ocker, B., Köhler, G., & Lamers, M. (1997). CD22 is a negative regulator of B-cell receptor signalling. *Current Biology*, *7*(2), 133–143. https://doi.org/10.1016/S0960-9822(06)00057-1

Nomura, K., Vilalta, A., Allendorf, D., Hornik, T., & Brown, G. (2017). Activated microglia desialylate and phagocytose cells via neuraminidase, galectin-3, and Mer tyrosine kinase. *The Journal of Immunology*, *198*(12), 4792–4801. https://doi.org/10.4049/jimmunol.1502532

Palecek, S., Loftus, J., Ginsberg, M., Lauffenburger, D., & Horwitz, A. (1997). Integrin-ligand binding properties govern cell migration speed through cell-substratum adhesiveness. *Nature*, *385*(6616), 537–540.

Papageorgiou, I., Loken, M., Brodersen, L., Gbadamosi, M., Uy, G., Meshinchi, S., & Lamba, J. (2019). CCGG deletion (rs201074739) in CD33 results in premature termination codon and complete loss of CD33 expression: Another key variant with potential impact on response to CD33-directed agents. *Leukemia & Lymphoma*, *60*(9), 2287–2290. https://doi.org/10.1080/10428194.2019.1569232

Paul, S., Taylor, L., Stansbury, E., & McVicar, D. (2000). Myeloid specific human CD33 is an inhibitory receptor with differential ITIM function in recruiting the phosphatases SHP-1 and SHP-2. *Blood*, *96*(2), 483–490.

Pluvinage, J., Haney, M., Smith, B., Sun, J., Iram, T., Bonanno, L., Li, L., Lee, D., Morgens, D., Yang, A., Shuken, S., Gate, D., Scott, M., Khatri, P., Luo, J., Bertozzi, C., Bassik, M., & Wyss-Coray, T. (2019). CD22 blockade restores homeostatic microglial phagocytosis in ageing brains. *Nature*, *568*(7751), 187–192. https://doi.org/10.1038/s41586-019-1088-4

Pugacheva, E. N., Roegiers, F., & Golemis, E. A. (2006). Interdependence of cell attachment and cell cycle signaling. *Current Opinion in Cell Biology*, 507–515. https://doi.org/10.1016/j.ceb.2006.08.014

Schmidt, S., & Friedl, P. (2010). Interstitial cell migration: Integrin-dependent and alternative adhesion mechanisms. *Cell and Tissue Research*, *339*(1), 83–92. https://doi.org/10.1007/s00441-009-0892-9

Schwartz, M., & Assoian, R. (2001). Integrins and cell proliferation: Regulation of cyclindependent kinases via cytoplasmic signaling pathways. *Journal of Cell Science*, *114*(14), 2553–2560.

Siddiqui, S., Springer, S., Verhagen, A., Sundaramurthy, V., Alisson-Silva, F., Jiang, W., Ghosh, P., & Varki, A. (2017). The Alzheimer's disease–protective CD33 splice variant mediates adaptive loss of function via diversion to an intracellular pool. *Journal of Biochemistry*, *292*(37), 15312–15320. https://doi.org/10.1074/jbc.M117.799346

Spangenberg, E., Lee, R., Najafi, A., Rice, R., Elmore, M., Blurton-Jones, M., West, B., & Green, K. (2016). Eliminating microglia in Alzheimer's mice prevents neuronal loss without modulating amyloid-β pathology. *Brain*, *139*(4), 1265–1281. https://doi.org/10.1093/brain/aww016

Sudom, A., Talreja, S., Danao, J., Bragg, E., Kegel, R., Min, X., Richardson, J., Zhang, Z., Sharkov, N., Marcora, E., Thibault, S., Bradley, J., Wood, S., Lim, A., Chen, H., Wang, S., Foltz, I., Sambashivan, S., & Wang, Z. (2018). Molecular basis for the loss-of-function effects of the Alzheimer's disease–associated R47H variant of the immune receptor TREM2. *Journal of Biochemistry*, *293*(32), 12634–12646. https://doi.org/10.1074/jbc.RA118.002352

Takahashi, K., Prinz, M., Stagi, M., Chechneva, O., & Neumann, H. (2007). TREM2-transduced myeloid precursors mediate nervous tissue debris clearance and facilitate recovery in an animal model of multiple sclerosis. *PLoS Med*, *4*(4), 675–689. https://doi.org/10.1371/journal.pmed.0040124

Takahashi, K., Rochford, C. D. P., & Neumann, H. (2005). Clearance of apoptotic neurons without inflammation by microglial triggering receptor expressed on myeloid cells-2. *Journal of Experimental Medicine*, *201*(4), 647–657.

Taylor, V., Buckley, C., Douglas, M., Cody, A., Simmons, D., & Freeman, S. (1999). The myeloid-specific Sialic acid-binding receptor, CD33, associates with the protein-tyrosine phosphatases, SHP-1 and SHP-2. *Journal of Biochemistry*, *274*(17), 11505–11512. https://doi.org/10.1074/jbc.274.17.11505

Tchilian, E., Beverley, P., Young, B., & Watt, S. (1994). Molecular cloning of two isoforms of the murine homolog of the myeloid CD33 antigen. *Blood*, *83*(11), 3188–3198. https://doi.org/10.1182/blood.V83.11.3188.3188

Ulyanova, T., Blasioli, J., Woodford-Thomas, T., & Thomas, M. (1999). The sialoadhesin CD33 is a myeloid-specific inhibitory receptor. *European Journal of Immunology*, *29*(11), 3440–3449. https://doi.org/10.1002/(SICI)1521-4141(199911)29:11<3440:AID-IMMU3440>3.0.CO;2-C

Vilalta, A., & Brown, G. C. (2018). Neurophagy, the phagocytosis of live neurons and synapses by glia, contributes to brain development and disease. *FEBS Journal*, *285*(19), 3566–3575. https://doi.org/10.1111/febs.14323

Vitale, C., Romagnani, C., Falco, M., Ponte, M., Vitale, M., Moretta, A., Bacigalupo, A., Moretta, L., & Mingari, M. (1999). Engagement of p75/AIRM1 or CD33 inhibits the proliferation of normal or leukemic myeloid cells. *PNAS*, *96*(26), 15091–15096. https://doi.org/10.1073/pnas.96.26.15091

Walter, R., Häusermann, P., Raden, B., Teckchandani, A., Kamikura, D., Bernstein, I., & Cooper, J. (2007). Phosphorylated ITIMs enable

ubiquitylation of an inhibitory cell surface receptor. *Traffic*, *9*(2), 267–279.

Wolf, S. A., Boddeke, H. W. G. M., & Kettenmann, H. (2017). Microglia in physiology and disease. *Annu. Re. Physiol.*, *79*(1), 619–643.

SUPPORTING INFORMATION

Additional supporting information may be found online in the Supporting Information section.

How to cite this article: Ann Butler C, Thornton P, Charles Brown G. CD33M inhibits microglial phagocytosis, migration and proliferation, but the Alzheimer's disease-protective variant CD33m stimulates phagocytosis and proliferation, and inhibits adhesion. *J Neurochem*. 2021;158:297–310. https://doi.org/10.1111/jnc.15349